

Measurements of γ from tree-level decays

A. Bertolin

on behalf of the LHCb Collaboration

Istituto Nazionale di Fisica Nucleare, Sezione di Padova, Italy

The LHCb approach for a precise determination of the CKM angle γ from tree-level decays is presented. Up to 16 independent determinations, using a variety of beauty and charm mesons decay modes, are available at LHCb. Not all of them have the same sensitivity to γ . The best accuracy is reached by combining all of the available results. These proceedings review some of the independent determinations used in the combination and present the latest combined result available, as of Summer 2018.

I. INTRODUCTION

Following the arguments developed in [1], one of the mandatory requirements to understand the origin of the baryon asymmetry of the Universe is that both charge (C) and charge-parity (CP) symmetries are broken. The latter phenomenon arises in the Standard Model (SM) of particle physics through the complex phase of the Cabibbo-Kobayashi-Maskawa (CKM) quark mixing matrix, although the effect in the SM is not large enough to account for the observed baryon asymmetry in the Universe. Violation of CP symmetry can be studied by measuring the angles of the CKM unitarity triangle. One of these angles, $\gamma \equiv \arg(-V_{ud}V_{ub}^*/V_{cd}V_{cb}^*)$, can be measured using only tree-level processes; a method that, assuming new physics is not present in tree-level decays, has negligible theoretical uncertainty. Disagreement between such direct measurements of γ and the value inferred from global CKM fits, assuming the validity of the SM, would indicate new physics beyond the SM. The value of γ can be determined by exploiting the interference between favoured $b \rightarrow cW$ (V_{cb}) and suppressed $b \rightarrow uW$ (V_{ub}) transition amplitudes. The most precise way to determine γ is through a combination of measurements from many decay modes. Up to 16 decay modes are considered at present by the LHCb Collaboration [2]. Three of them, using very different analysis techniques, will be briefly discussed in the next sections. The last but one section will present the results of the combination. The last will draw conclusions and future prospects.

II. $B^+ \rightarrow DK^+(D \rightarrow K_S^0 h^+ h^-)$ ANALYSIS

In the decay mode $B^+ \rightarrow DK^+(D \rightarrow K_S^0 h^+ h^-)$, where D represents a neutral charm meson that is a mixture of the D^0 and \bar{D}^0 flavour eigenstates and h a π or a K meson, the sensitivity to γ is obtained comparing the D meson Dalitz plot distribution for reconstructed B^+ and B^- decays [3]. The $B^- \rightarrow DK^-$ decay amplitude can be written as:

$$A_B(m_-^2, m_+^2) \propto A_D(m_-^2, m_+^2) +$$

$$r_B e^{i(\delta_B - \gamma)} A_{\bar{D}}(m_-^2, m_+^2)$$

a sum of a favoured, the first, and a suppressed, the latter, amplitudes, where m_{\pm}^2 represents the $K_S^0 h^{\pm}$ invariant mass squared and r_B (δ_B) is the ratio (strong phase difference) between these amplitudes. Here and in the following the quantities labeled just r_B and δ_B are unique to each B decay mode. Four CPV observables defined as:

$$x_{\pm} \equiv r_B \cos(\delta_B \pm \gamma) \text{ and } y_{\pm} \equiv r_B \sin(\delta_B \pm \gamma)$$

are determined by measuring the B^+ and B^- yields in bins of the Dalitz plot variables m_+^2 and m_-^2 . The strong phase difference between the D^0 and \bar{D}^0 amplitudes at a given point of the Dalitz plot is also needed. This phase difference is being directly measured by the CLEO collaboration exploiting quantum-correlated $D^0 \bar{D}^0$ pairs produced at the $\psi(3770)$ resonance [4]. This approach makes the measurement independent of modelling the D decay amplitude. The D -decay Dalitz plot is partitioned into $2 \times N$ bins labelled from $i = -N$ to $i = +N$ (excluding zero), symmetric around $m_-^2 = m_+^2$ such that if (m_-^2, m_+^2) is in bin i then (m_+^2, m_-^2) is in bin $-i$. By convention, the positive values of i correspond to bins for which $m_-^2 > m_+^2$. The partition was chosen to optimise the statistical sensitivity to γ . The $B^{\pm} \rightarrow DK^{\pm}$ invariant mass distributions obtained in bin -4 and 4, using $D \rightarrow K_S^0 \pi^+ \pi^-$ and the 2015–2016 LHCb data are shown in Fig. 1: a clear asymmetry is visible. The data points are fitted using a signal and several background components. Overall a yield of about 2000 events is observed for each of $B^- \rightarrow DK^-$ and $B^+ \rightarrow DK^+$. The difference in the B^+ and B^- yields

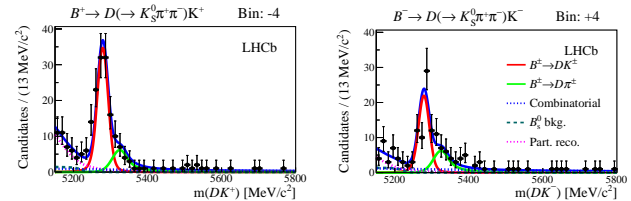


FIG. 1: Invariant mass distributions of (left) $B^+ \rightarrow DK^+$ and (right) $B^- \rightarrow DK^-$ in bin -4 and 4, respectively. Reproduced from Ref. [3].

as a function of this effective bin number is shown in Fig. 2. Dots represent data, the dotted line the expectation without CPV and the continuous line the fit prediction with the central values of the parameters x_{\pm} and y_{\pm} . A graphical representation of the x_{\pm} and

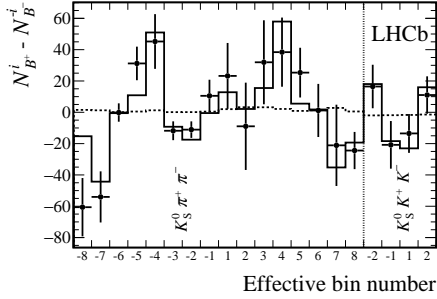


FIG. 2: Difference in the B^+ and B^- yields as a function of the effective bin number. Reproduced from Ref. [3].

y_{\pm} values in terms of γ is given in Fig. 3, corresponding to:

$$\gamma = (87_{-12}^{+11})^\circ$$

where the uncertainty corresponds to the 68 % confidence interval. This is the most precise determination of γ from a single analysis. At present the result is statistically limited but the analysis presented was using only 2015–2016 data, so only 2 out of the 5.9 fb^{-1} available in Run2.

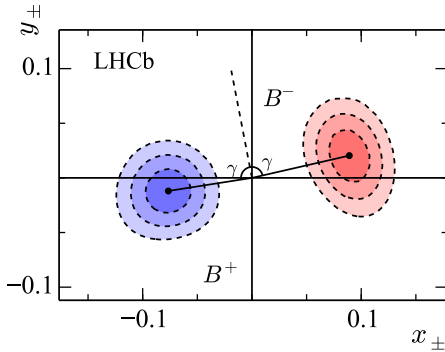


FIG. 3: Graphical representation of the x_{\pm} and y_{\pm} values in terms of γ . The 68.2 %, 95.5 % and 99.7 % probability regions for x_{\pm} and y_{\pm} are represented by the dashed areas. Reproduced from Ref. [3].

III. $B^+ \rightarrow DK^{*+}$ (2, 4 BODY D DECAYS) ANALYSIS

In the decay mode $B^+ \rightarrow DK^{*+}$, where the neutral D meson decays to h^+h^- and $h^+\pi - \pi + \pi^-$, $h = K, \pi$ and the K^{*+} meson to $K_S^0\pi^+$, the sensitivity to γ is obtained from the interference observed by

reconstructing the D meson in final states accessible to both D^0 and \bar{D}^0 [5]. Up to 12 CP observables can be measured. For illustration purposes, one of them is defined as:

$$A_{KK} \equiv \frac{\Gamma(B^- \rightarrow D(K^+K^-)K^{*-}) - \Gamma(B^+ \rightarrow D(K^+K^-)K^{*+})}{\Gamma(B^- \rightarrow D(K^+K^-)K^{*-}) + \Gamma(B^+ \rightarrow D(K^+K^-)K^{*+})}$$

which represents the CP asymmetry for the $D \rightarrow K^+K^-$ decay mode. $A_{\pi\pi}$ is defined similarly but swapping K^+K^- with $\pi^+\pi^-$. As direct CP violation in D decay is small $A_{KK} = A_{\pi\pi} \equiv A_{CP+}$ where

$$A_{CP+} = \frac{2kr_B \sin \delta_B \sin \gamma}{1 + r_B^2 + 2kr_B \cos \delta_B \cos \gamma}$$

with r_B and δ_B defined as in the previous section and k a dilution factor for non $K^*(892)^- \rightarrow K_S^0\pi^-$ contributions. This shows the connection, for one of the 12 CP observables, with the physical parameter of interest, γ . The observed invariant mass distribution for $B^- \rightarrow D(K^+K^-)K^{*-}$ is shown in the left plot of Fig. 4 with the charge conjugated process on the right. Overall, 7 different D decay modes are consid-

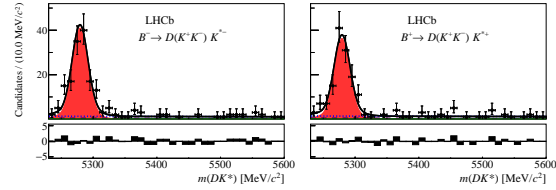


FIG. 4: Observed invariant mass distribution for (right) $B^- \rightarrow D(K^+K^-)K^{*-}$ and (left) $B^+ \rightarrow D(K^+K^-)K^{*+}$. Reproduced from Ref. [5].

ered with the observed yields in the B^+ and B^- cases reported in Tab. I. The analysis is using the 2011 to 2016 LHCb data set. These numbers allow the ex-

TABLE I: B^+ and B^- measured yields for each of the 7 considered D decay modes. Reproduced from Ref. [5].

Decay mode	B^- yield	B^+ yield
$B^\pm \rightarrow D(K^\pm\pi^\mp)K^{*\pm}$	996 ± 34	1035 ± 35
$B^\pm \rightarrow D(K^+K^-)K^{*\pm}$	134 ± 14	121 ± 13
$B^\pm \rightarrow D(\pi^+\pi^-)K^{*\pm}$	45 ± 10	33 ± 9
$B^\pm \rightarrow D(K^\mp\pi^\pm)K^{*\pm}$	1.6 ± 1.9	19 ± 7
$B^\pm \rightarrow D(K^\pm\pi^\mp\pi^+\pi^-)K^{*\pm}$	556 ± 26	588 ± 27
$B^\pm \rightarrow D(\pi^+\pi^-\pi^+\pi^-)K^{*\pm}$	59 ± 10	56 ± 10
$B^\pm \rightarrow D(K^\mp\pi^\pm\pi^-\pi^+)K^{*\pm}$	3 ± 5	10 ± 6

traction of the 12 CP observables. For illustration purposes:

$$A_{KK} = -0.004 \pm 0.023 \pm 0.008$$

$$A_{\pi\pi} = 0.15 \pm 0.13 \pm 0.02$$

where the first uncertainty is statistical and the second systematic. As anticipated, within the present uncertainties, A_{KK} and $A_{\pi\pi}$ are indeed equal. Please see Ref. [5] for a full summary of the results. The physical interpretation in term of r_B and γ , using the full set of CP observables, is given in Fig. 5. Along this particu-

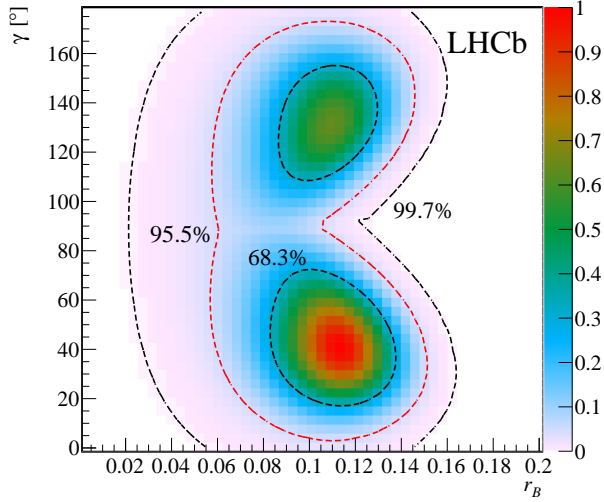


FIG. 5: r_B vs γ allowed region using the values of the 12 CP observables from $B^\pm \rightarrow DK^{*\pm}$. Reproduced from Ref. [5].

lar decay mode has a limited sensitivity but results are consistent with $\gamma \sim 70^\circ$ and $r_B \sim 0.1$. Measurements are statistically limited but statistic will increase from 5.2 to 9.1 fb^{-1} once the 2017 and the 2018 data samples are included.

IV. $B_s^0 \rightarrow D_s K$ ANALYSIS

In the decay mode $B_s^0 \rightarrow D_s^\mp K^\pm$ the sensitivity to γ is obtained from the interference of decay amplitudes with and without mixing [6]. This is a time dependent analysis requiring flavour tagging to determine the flavour of the reconstructed neutral B meson at production time. The CP parameters related to r_B , δ_B and $(\gamma - 2\beta_s)$, where $\beta_s \equiv \arg(-V_{ts}V_{tb}^*/V_{cs}V_{cb}^*)$, are obtained fitting the observed decay time distribution. The fit results to the $D_s^\mp K^\pm$ invariant mass distribution are illustrated in Fig. 6. Using the 2011–2012 data sample a signal yield of 5955 ± 90 is obtained. The observed decay time distribution is shown in Fig. 6. The red dashed line in the same figure corresponds to the decay time acceptance as obtained from $B_s^0 \rightarrow D_s^- \pi^+$ data after a small correction obtained from the $D_s^\mp K^\pm$ to $D_s^- \pi^+$ time acceptances ratio as obtained from Monte Carlo samples. The CPV parameters fit result is given by the blue continuous line.

PSN fpcpThuB1505

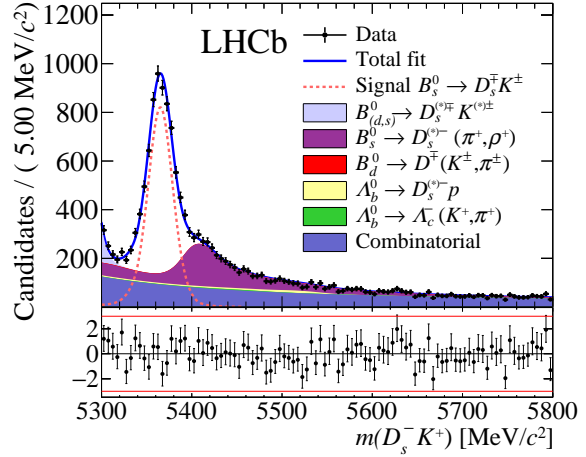


FIG. 6: $B_s^0 \rightarrow D_s^\mp K^\pm$ invariant mass distribution. Reproduced from Ref. [6].

As the effect of CPV is difficult to appreciate in Fig. 7, the folded time asymmetries for $D_s^+ K^-$ and $D_s^- K^+$ are shown in the left and right plots of Fig. 8, respectively. The effect of CPV can then be seen as a phase difference between the two asymmetries different from π at $t = 0$ ps. The final result for γ from this analysis being:

$$\gamma = (128_{-22}^{+17})^\circ.$$

This is the most precise determination of γ from a B_s meson decay. The result is obtained using so far only the 3 fb^{-1} collected in 2011–2012 and will be extended to the 5.9 fb^{-1} collected during Run2 allowing to improve significantly the statistical accuracy on γ .

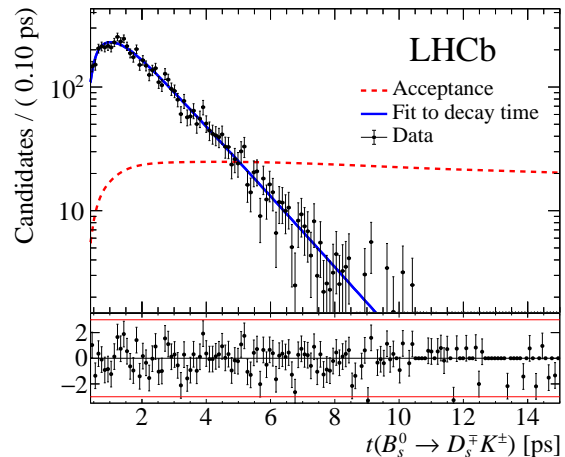


FIG. 7: Fit to the $B_s^0 \rightarrow D_s^\pm K^\mp$ observed decay time distribution. Reproduced from Ref. [6].

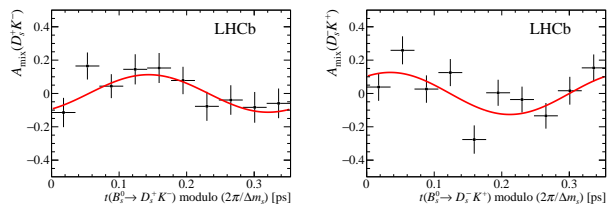


FIG. 8: Folded time asymmetry for (left) $D_s^+ K^-$ and (right) $D_s^- K^+$. Reproduced from Ref. [6].

V. γ COMBINATION RESULTS

As the most precise determination of γ from a single measurement presently has a statistical uncertainty around 10° , which is large with respect to what desirable, it is mandatory to combine the measurements obtained from all the accessible decay modes [2]. The present LHCb γ combination uses as input 98 observables to constrain 40 free parameters. The main results of the fit are γ , treated as a common free parameter, and the r_B and δ_B values of each considered decay mode. In order to extract γ from the measurements presented in the previous sections some "auxiliary" inputs are also needed. One example being the value of β_s for the $B_s^0 \rightarrow D_s K$ measurement. Whenever possible these auxiliary inputs are taken from data, whenever possible from LHCb data. These are Gauss-constrained in the combination. Treating them as free parameters roughly doubles the uncertainty on γ . The combination result for γ is:

$$\gamma = (74.0_{-5.8}^{+5.0})^\circ$$

where the accuracy increases by a factor of about 2 with respect to the most accurate single measurement. The 1-CL curve for the γ parameter is shown in Fig. 9 with central value (solid vertical line) and 1σ uncertainties (dashed vertical lines) labelled. The 1 and 2σ levels are indicated by the horizontal dotted lines. B^+ , B^0 and the single B_s^0 meson results are currently used in the γ combination, the corresponding 1-CL curves are shown in violet, yellow and orange in Fig. 10, respectively. The green curve shows the combination is as in Fig. 9. Such a "differential" analysis allows to probe the stability and the strength of the result. B^+ are clearly driving the final result. B^0 and B_s^0 are subdominant and having almost the same weight. This happens because the r_B value of the single B_s^0 measurement is 0.301, the largest measured so far. Future measurements using $B_c^\pm \rightarrow D_s^\pm D$, the analogue of $B_s^0 \rightarrow D_s^\pm K^\mp$ replacing the s quark with a b quark, penalized by a small production yield, are expected to have $r_B \sim O(1)$ [7].

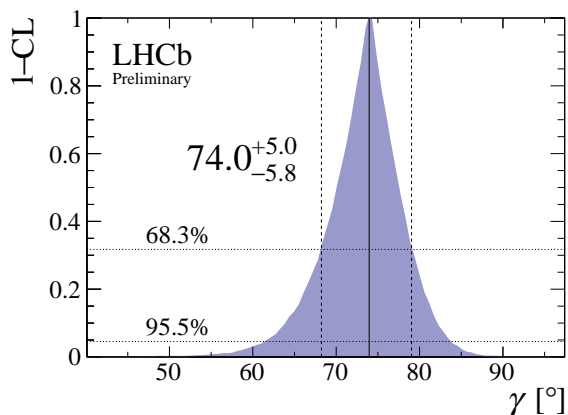


FIG. 9: 1-CL curve for the γ combination. Reproduced from Ref. [2].

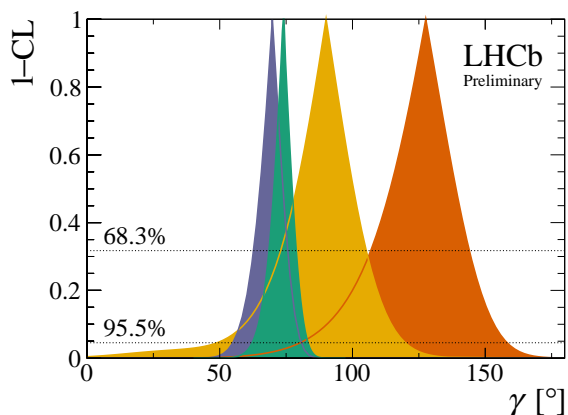


FIG. 10: 1-CL plots for combinations split by the initial B meson flavour. Reproduced from Ref. [2].

VI. SUMMARY AND FUTURE PROSPECTS

The result of the 2018 LHCb γ combination is:

$$\gamma = (74.0_{-5.8}^{+5.0})^\circ$$

based on 16 input measurements that cross check each other and allow to evaluate the stability of the combined result. This value is compared in Fig. 11 with the CKMfitter [8] and UTfit [9] global fit results, as of Summer 2018. Clearly the present LHCb uncertainty on γ does not yet allow to draw any stringent conclusion from the comparison between tree-level and global fits determinations. On a short term time scale LHCb will extend all input measurements to the full Run1 plus Run2 data set. In addition new measurements are about to come at the time these proceedings are being written. Longer term, starting from about 2021, new data will be available thanks to the high luminosity LHC upgrade. With possibly additional inputs to the combination. Current projections

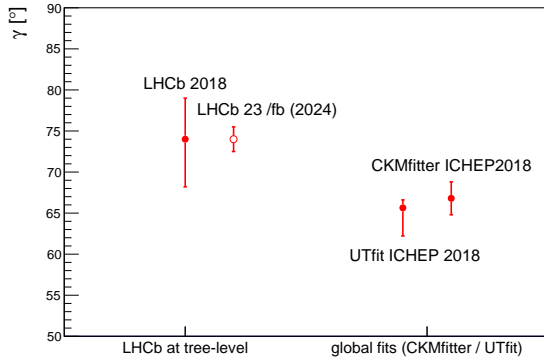


FIG. 11: Comparison between the present LHCb γ result from tree-level decays and the global fit determinations from CKMfitter and UTfit. A projection of the LHCb γ result based on the data sample that will be collected by 2024, after the high luminosity LHC upgrade, is also shown.

indicate that with a luminosity of 23 fb^{-1} , available by about 2024, an accuracy of 1.5° should be reachable. As shown in Fig. 11, at that time the LHCb uncertainty will be similar to the present global fits uncertainty (in Fig. 11 the central value of the expected 23 fb^{-1} result has been arbitrarily kept to its current value). If the accuracy of the external inputs will not limit the LHCb measurements and if a luminosity of 300 fb^{-1} could be reached by the end of LHC operations the uncertainty on γ should shrink to 0.35° . At present LHCb has improved the accuracy of the γ measurement obtained by BaBar or Belle by a factor of about 3. In the forthcoming months Belle II, that started full physics operation in 2019, will start to push towards a reduction of the uncertainty on γ , having about the same expected sensitivity as LHCb.

-
- [1] R. Aaij *et al.* (LHCb Collaboration), JHEP12 (2016) 087.
- [2] R. Aaij *et al.* (LHCb Collaboration), LHCb-CONF-2018-002, Conference report prepared for BEAUTY 2018, 6th–11th May 2018, Elba.
- [3] R. Aaij *et al.* (LHCb Collaboration), JHEP08 (2018) 176.
- [4] J. Libby *et al.* (CLEO Collaboration), Phys. Rev. D **82**, 112006 (2010).
- [5] R. Aaij *et al.* (LHCb Collaboration), JHEP11 (2017) 156.
- [6] R. Aaij *et al.* (LHCb Collaboration), JHEP03 (2018) 059.
- [7] A. K. Giri, R. Mohanta, and M. P. Khanna, Phys. Rev. D **65**, 034016 (2002).
- [8] http://ckmfitter.in2p3.fr/www/results/plots_summer18/ckm_res_summer18.html
- [9] <http://www.utfit.org/UTfit/ResultsSummer2018SM>